Supporting Information

Enhancing Near-Infrared Photothermal Activity through Precise In-Plane Interface Engineering in CuS-Au and CuS@Au Ultrathin Nanoplates for Combating Multidrug-Resistant Bacteria

Yuxin Wu,[a†] Qi He,[b†] Heng Zhang,[c†] Xiaolin Meng,[d†] Yuanyuan Min,[a] Yi Wang,[b*] Xiaohu Wu,[e*] Pu Zhang,[d*] Yanyun Ma,[f] and Yiqun Zheng[a*]

[a] School of Chemistry, Chemical Engineering, and Materials, Jining University, Qufu, Shandong 273155, P. R. China
[b] Chongqing Key Laboratory of Green Synthesis and Applications, College of Chemistry, Chongqing Normal University, Chongqing 401331, China
[c] School of Energy, Changzhou University, Changzhou, Jiangsu 213164, P. R. China
[d] Chongqing Research Center for Pharmaceutical Engineering, College of Pharmacy, Chongqing Medical University, Chongqing 400016, P. R. China
[e] Thermal Science Research Center, Shandong Institute of Advanced Technology, Jinan, Shandong 250100, China
[f] Institute of Functional Nano & Soft Materials (FUNSOM), Jiangsu Key Laboratory for Carbon-Based Functional Materials & Devices, Soochow University, Suzhou, Jiangsu 215123, P. R. China

[†] These authors contributed equally to this work.
[*] Corresponding authors: Prof. Dr. Y. Zheng, E-mail: yzheng@jnxy.edu.cn; Prof. Dr. Y. Wang, E-mail: ywang@cqnu.edu.cn; Prof. X. Wu, xiaohu.wu@iat.cn; Prof. P. Zhang, zhangpu@cqmu.edu.cn

Calculation of the Photothermal Transduction Efficiency

The photothermal conversion efficiency (η) was calculated according to the formula Eq. S1 proposed by Roper:[1]

$$\eta = \frac{hA(\Delta T_{max} - \Delta T_{Solvent})}{I\,(1 - 10^{-A_\lambda})} \times 100\% \quad \text{(Eq. S1)}$$

where h is the heat transfer coefficient, A is the surface area for radiative heat transfer, ΔT_{max} represents the maximum steady-state temperature in the presence of products relative to room temperature, $\Delta T_{solvent}$ represents the maximum steady-state temperature of solvent relative to room temperature, I is the power density of used laser, and A_λ is the absorbance of products at 808 or 1064 nm.

References

1. D. K. Roper, W. Ahn and M. Hoepfner, *J. Phys. Chem. C*, 2007, **111**, 3636-3641.

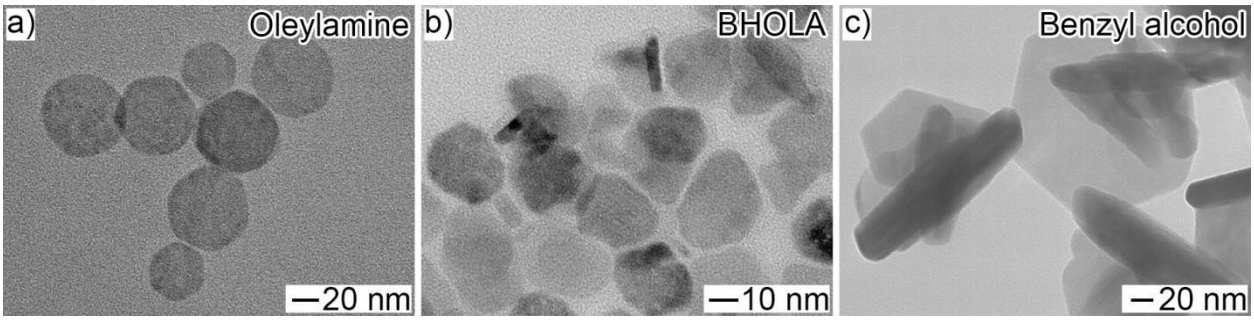

Figure S1. TEM images of CuS products obtained *via* the standard procedure, except that the OPDA was replaced by a) oleylamine, b) bis(2-hydroxyethy) oleylamine (BHOLA), c) benzyl alcohol, respectively.

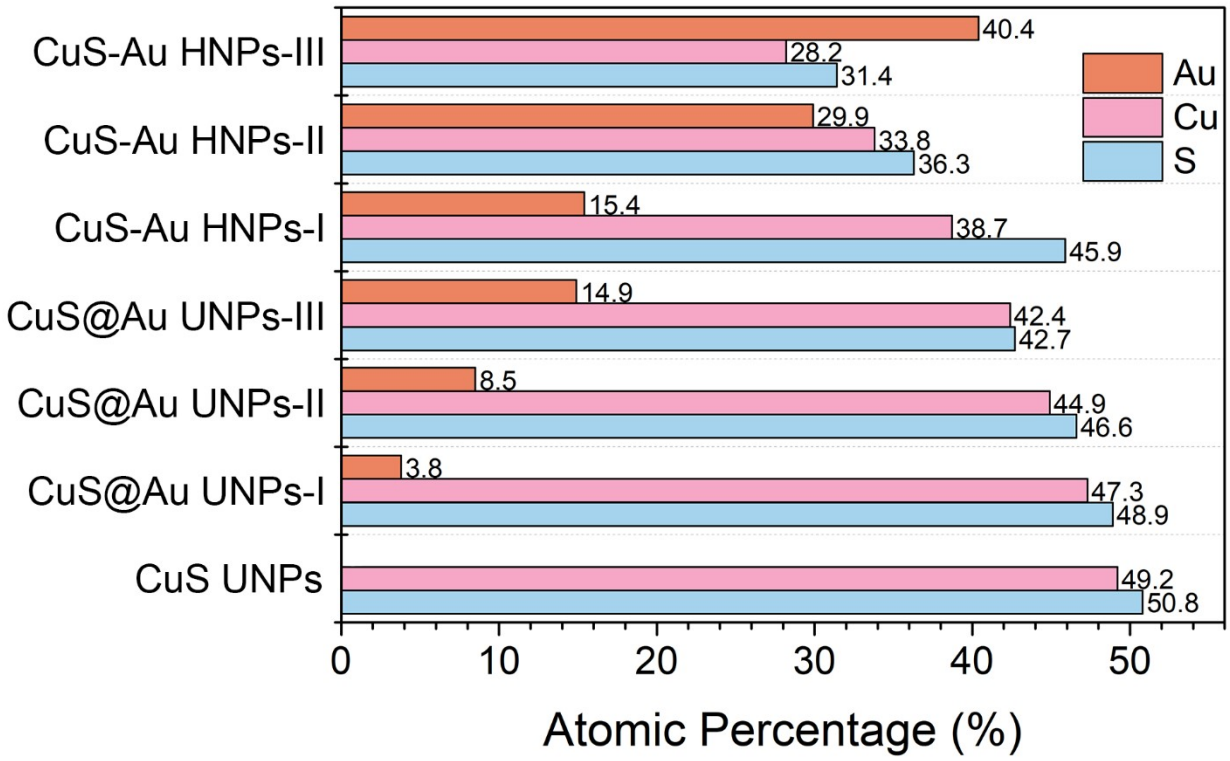

Figure S2. EDS histograms showing the elemental composition of CuS-based products shown in Figure 1 and Figure 2.

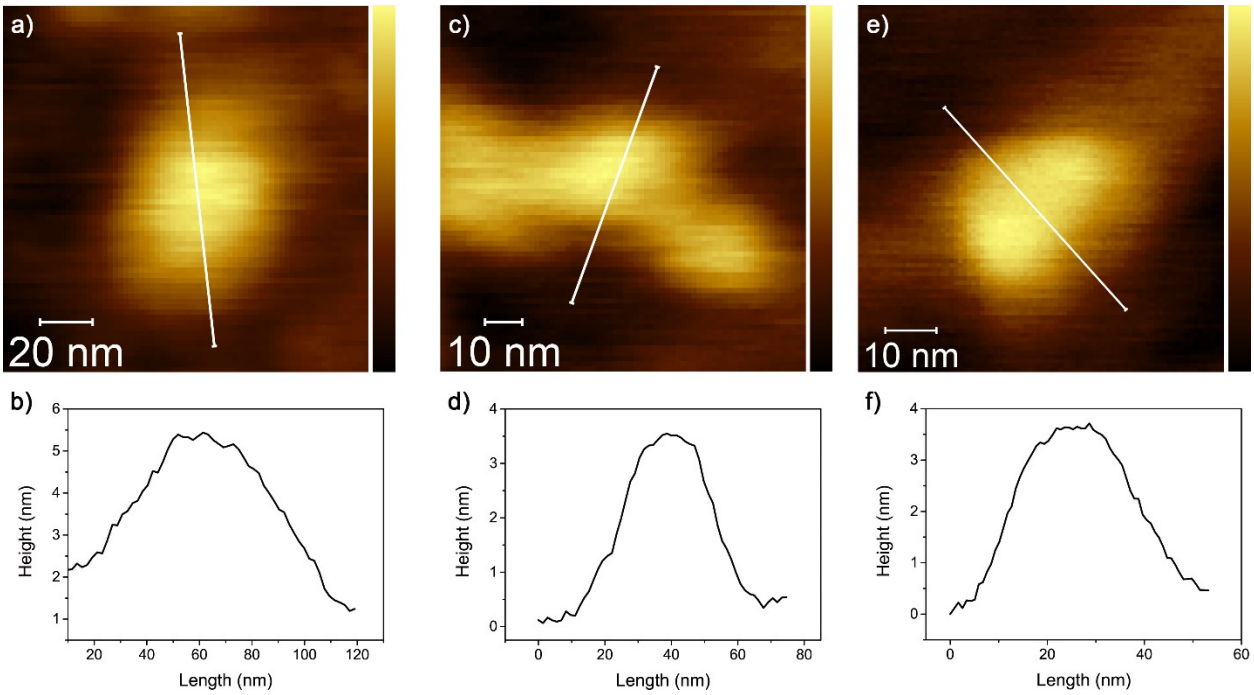

Figure S3. a, c, e) AFM images and b, d, f) corresponding height profiles of a, b) CuS UNPs, c, d) CuS@Au UNPs-II and e, f) CuS-Au HNPs-I.

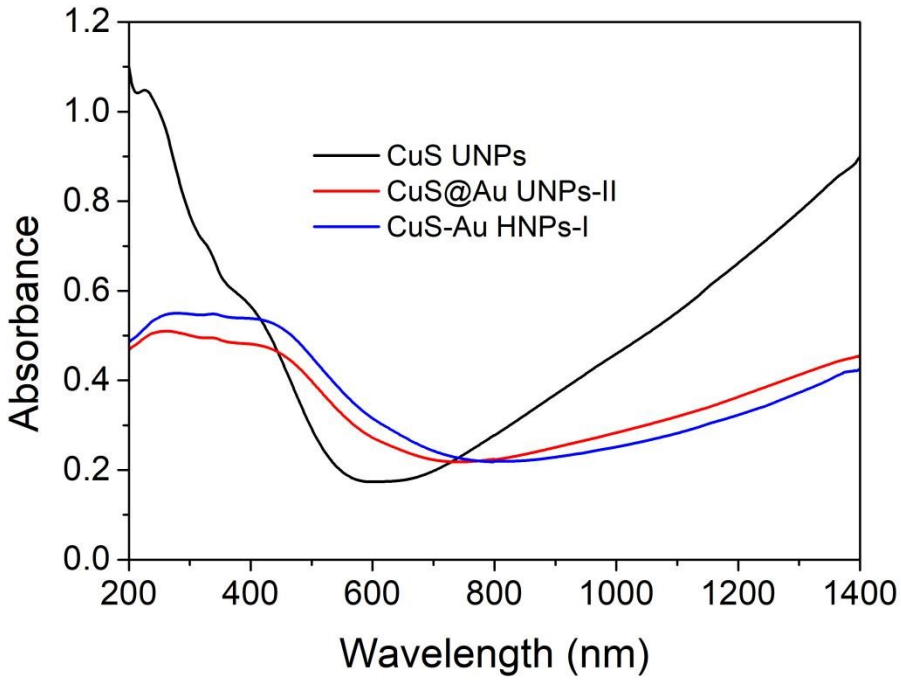

Figure S4. UV−vis−NIR extinction spectra of aqueous suspensions containing CuS UNPs, CuS@Au UNPs-II and CuS-Au HNPs-I.

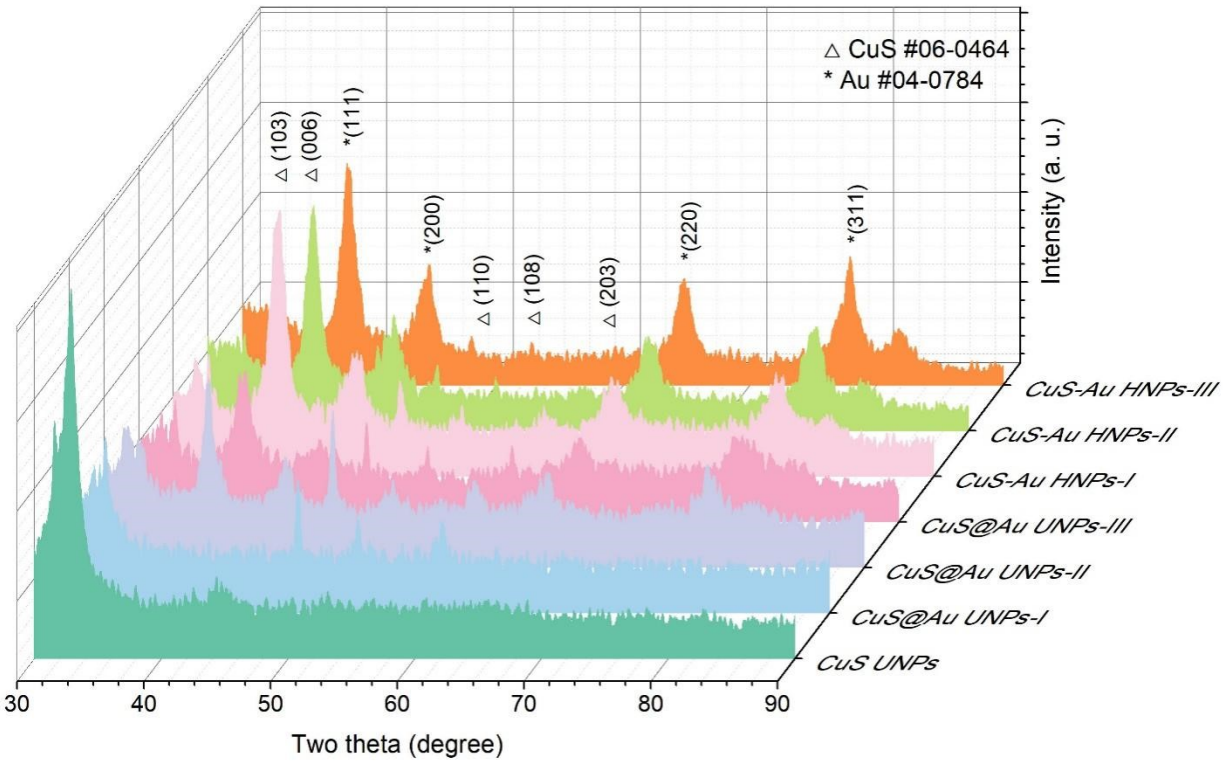

Figure S5. X-Ray diffraction (XRD) patterns of CuS UNPs, CuS@Au UNPs and CuS-Au HNPs.

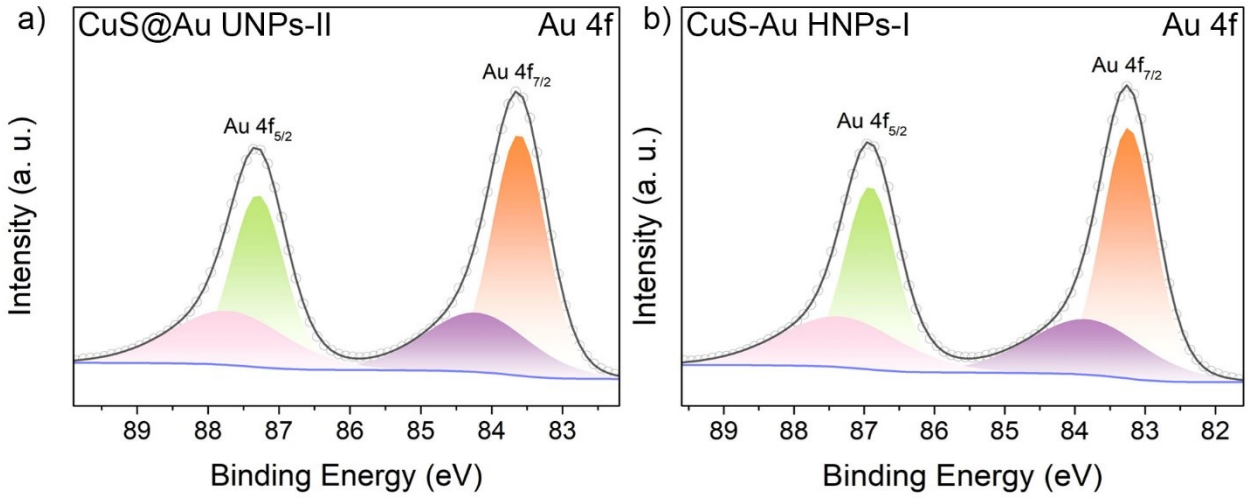

Figure S6. High-resolution Au 4f spectra of a) CuS@Au UNPs-II and b) CuS-Au HNPs-I.

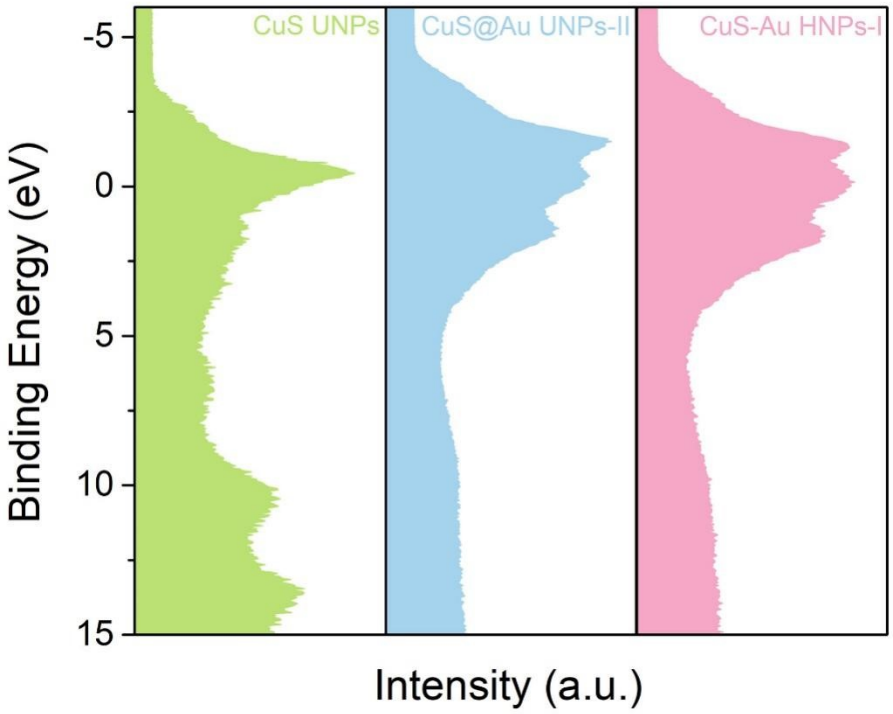

Figure S7. XPS valence band spectra measured for CuS UNPs, CuS@Au UNPs-II and CuS-Au HNPs-I.

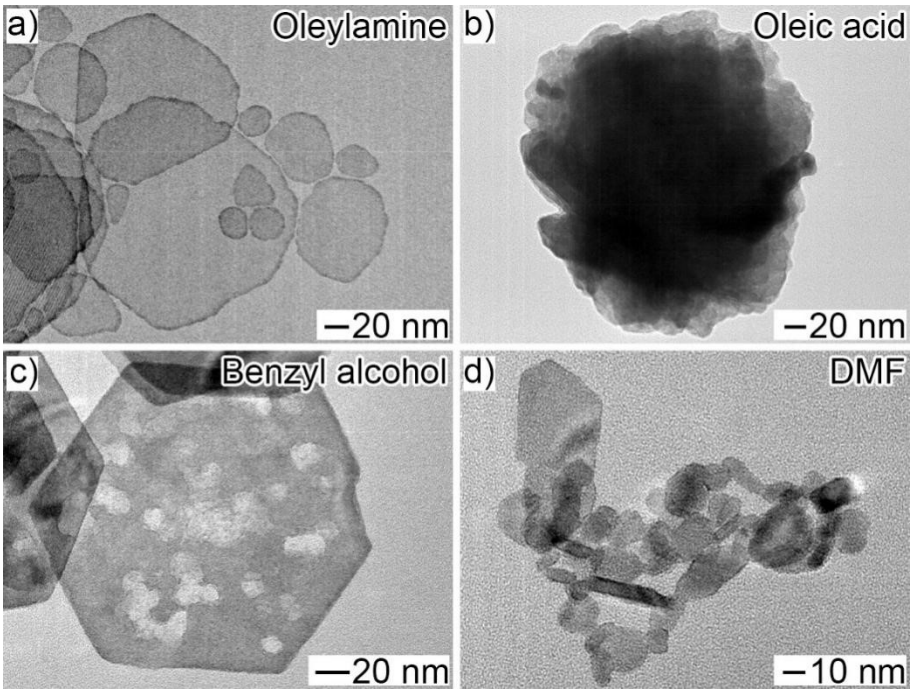

Figure S8. TEM image of CuS@Au products obtained *via* the standard procedure of CuS@Au UNPs-II, except that the OPDA was replaced by a) oleylamine, b) oleic acid, c) benzyl alcohol, d) N, N-dimethylformamide (DMF), respectively.

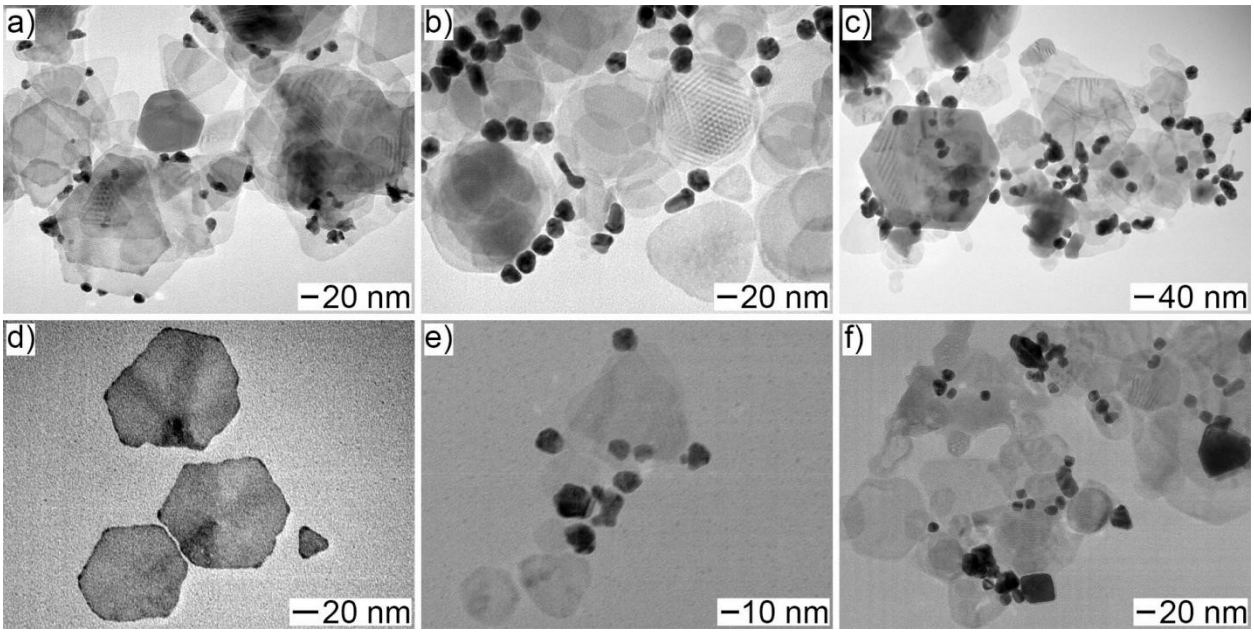

Figure S9. TEM images of CuS@Au and CuS-Au products obtained at variable conditions. See Table S6 for details.

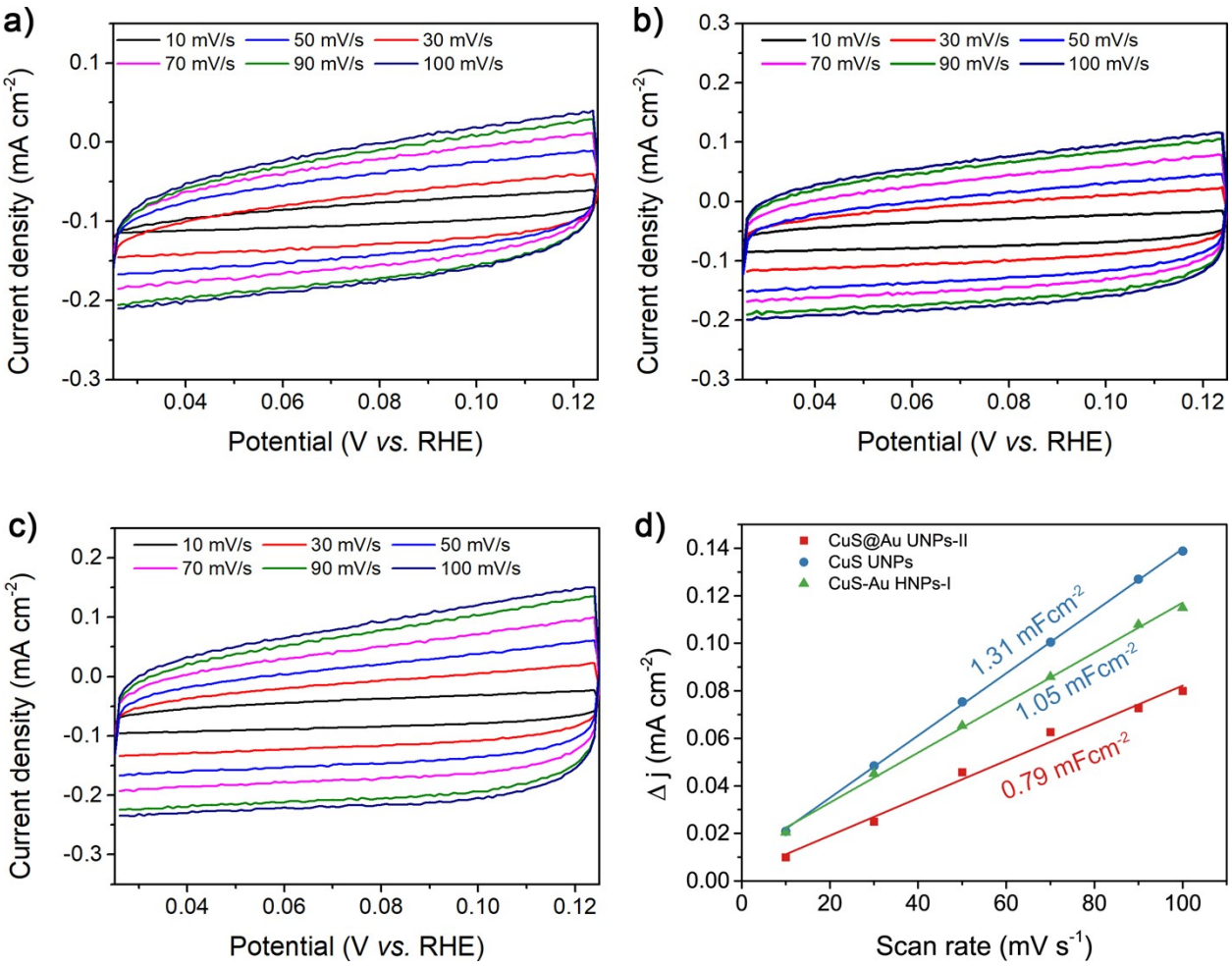

Figure S10. Cyclic voltammetry curves of a) CuS@Au UNPs-II, b) CuS-Au HNPs-I, and c) CuS UNPs at different scan rates ranging from 10 mV s^{-1} to 100 mV s^{-1} in 1 M KOH, d) C_{dl} curves as a function of scan rate ranging from 10 mV·s^{-1} to 100 mV·s^{-1}.

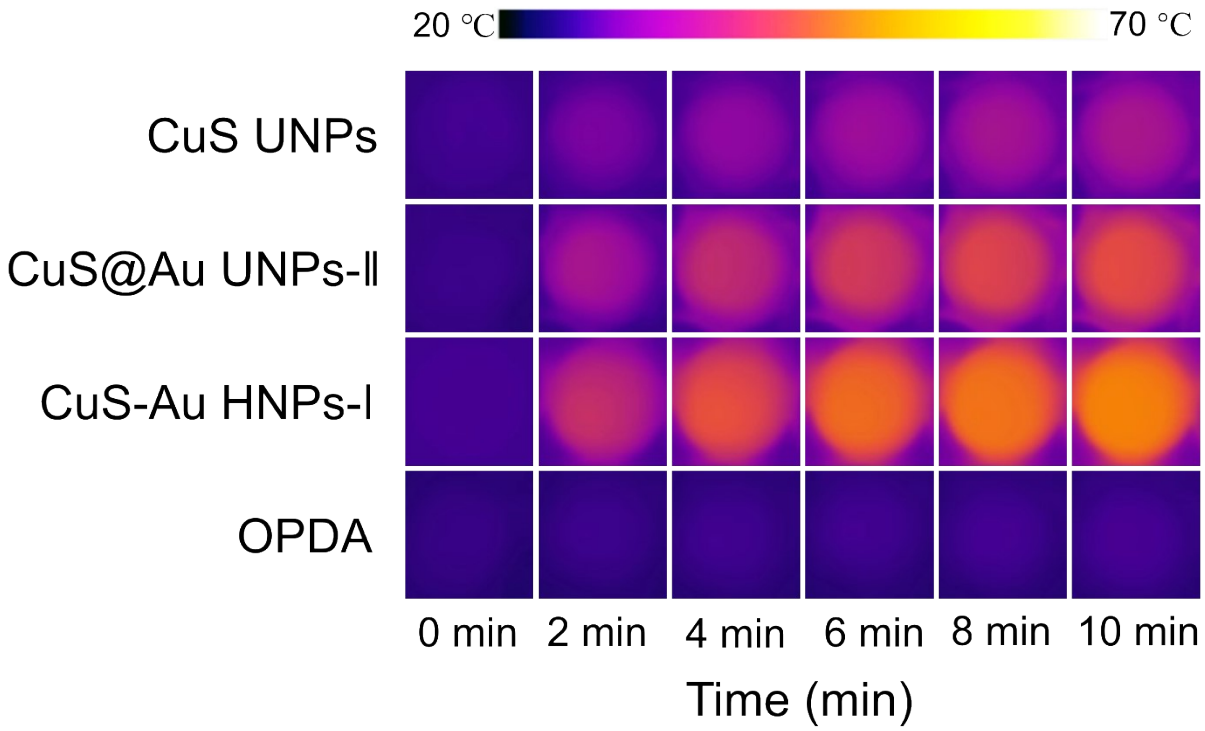

Figure S11. Photothermal IR images of three samples upon 808 nm irradiation.

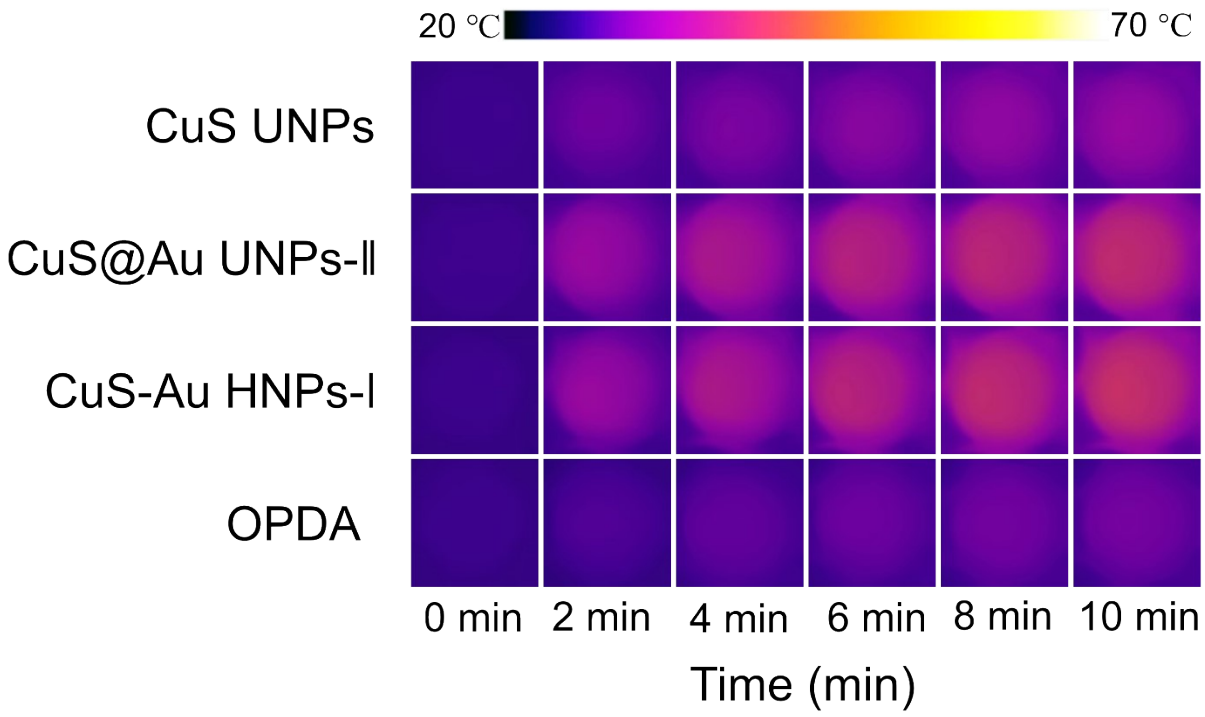

Figure S12. Photothermal IR images of three samples upon 1064 nm irradiation.

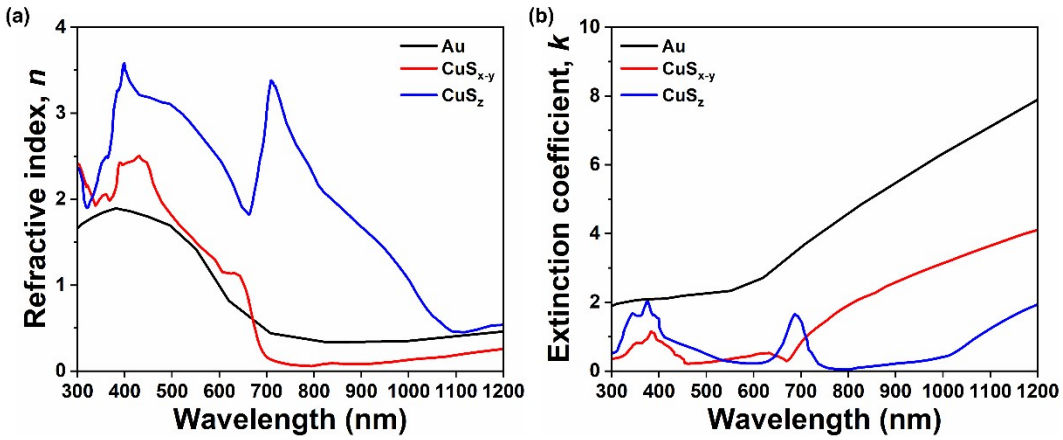

Figure S13. Optical parameters of the materials. (a) Refractive index, (b) extinction coefficient.

Table S1. Summary of size information of products in the current study.

Sample	Lateral size of plate (nm)		Thickness of edge (nm)		Diameter of dot (nm)	
	Average value	Standard deviation	Average value	Standard deviation	Average value	Standard deviation
CuS NSs	130	19.8	N/A	N/A	N/A	N/A
Figure 2b	83.7	17.0	1.94	0.73	N/A	N/A
Figure 2c	46.4	7.92	1.76	0.50	N/A	N/A
Figure 2d	43.7	6.51	3.21	0.82	3.26	1.53
Figure 2e	72.8	16.9	/	/	10.2	2.16
Figure 2f	61.7	16.7	/	/	9.75	2.05
Figure 2g	53.0	21.9	/	/	12.2	3.72

Table S2. Summary of synthetic parameters for CuS UNPs, CuS@Au UNPs, and CuS-Au HNPs shown in Figure 1 and 2.

Figure No.	Sample	$Cu(acac)_2$	S	OPDA	$HAuCl_4$
Figure 1	CuS UNPs	10 mg	10 mg	10 mL	0
Figure 2b	CuS@Au UNPs-I	10 mg	10 mg	10 mL	1.9 μmol
Figure 2c	CuS@Au UNPs-II	10 mg	10 mg	10 mL	3.8 μmol
Figure 2d	CuS@Au UNPs-III	10 mg	10 mg	10 mL	7.6 μmol
Figure 2e	CuS-Au HNPs-I	10 mg	10 mg	10 mL	9.5 μmol
Figure 2f	CuS-Au HNPs-II	10 mg	10 mg	10 mL	19 μmol
Figure 2g	CuS-Au HNPs-III	10 mg	10 mg	10 mL	38 μmol

Table S3. Summary of the relative peak areas (%) for each split B.E. peak and the parameters used to fit the Cu 2p and S 2p high-resolution XPS spectra of CuS UNPs.

Orbital	B. E. Peak (eV)	FWHM (eV)	peak area (%)	element/oxidation state
Cu 2p	931.8	1.15	23.02	Cu (0/I)
	933.2	3.60	26.61	Cu (0/I)
	951.8	1.93	12.80	Cu (0/I)
	953.5	9.90	37.57	Cu (0/I))
S 2p	161.6	1.31	19.11	S (-II)
	162.8	2.76	40.95	S (-II)
	167.9	1.39	28.07	S (-I)
	169.2	1.25	11.87	S (-I)

Table S4. Summary of the relative peak areas (%) for each split B.E. peak and the parameters used to fit the Cu 2p, S 2p and Au 4f high-resolution XPS spectra of CuS@Au UNPs-II.

Orbital	B. E. Peak (eV)	FWHM (eV)	peak area (%)	element/oxidation state
Cu 2p	931.7	0.98	21.55	Cu (0/I)
	932.5	2.91	25.42	Cu (0/I)
	947.6	15.1	23.41	Cu (0/I)
	951.6	1.62	12.73	Cu (0/I)
	953.5	5.37	16.89	Cu (0/I)
S 2p	160.7	0.68	7.12	S (-II)
	161.6	0.98	42.70	S (-II)
	162.7	0.92	19.98	S (-I)
	163.2	2.58	30.20	S (-I)
Au 4f	83.66	0.90	37.75	Au (0)
	84.26	1.74	17.89	Au (0)
	87.26	0.89	26.50	Au (0)
	87.76	1.90	17.86	Au (0)

Table S5. Summary of the relative peak areas (%) for each split B.E. peak and the parameters used to fit the Cu 2p, S 2p and Au 4f high-resolution XPS spectra of CuS-Au HNPs-I.

Orbital	B. E. Peak (eV)	FWHM (eV)	peak area (%)	element/oxidation state
Cu 2p	931.2	1.03	26.37	Cu (0/I)
	932.1	2.75	21.39	Cu (0/I)
	951.1	1.39	11.02	Cu (0/I)
	952.2	6.75	41.22	Cu (0/I)
S 2p	160.4	0.73	8.59	S (-II)
	161.2	0.89	39.01	S (-II)
	162.3	1.11	28.06	S (-I)
	162.9	2.64	24.34	S (-I)
Au 4f	83.26	0.89	37.77	Au (0)
	83.86	1.92	17.95	Au (0)
	86.96	0.87	27.08	Au (0)
	87.36	2.01	17.20	Au (0)

Table S6. Summary of synthetic parameters for CuS/Au products shown in Figure S11.

Sample	$Cu(acac)_2$	S	OPDA	$HAuCl_4$	Temperature (Step II)
Figure S10a	10 mg	10 mg	10 mL	1.9 μmol	60 °C
Figure S10b	10 mg	10 mg	10 mL	1.9 μmol	100 °C
Figure S10c	10 mg	10 mg	10 mL	1.9 μmol	150 °C
Figure S10d	10 mg	10 mg	10 mL	3.8 μmol	60 °C
Figure S10e	10 mg	10 mg	10 mL	3.8 μmol	100 °C
Figure S10f	10 mg	10 mg	10 mL	3.8 μmol	150 °C